

RESEARCH ARTICLE

High-Throughput Assay Development for Cystine-Glutamate Antiporter (x_c^-) Highlights Faster Cystine Uptake than Glutamate Release in Glioma Cells

Ajit G. Thomas¹, Rita Sattler^{1,2}, Karen Tendyke³, Kara A. Loiacono³, Hans Hansen³, Vishal Sahni⁴, Yutaka Hashizume⁴, Camilo Rojas^{1,5*}, Barbara S. Slusher^{1,2,6,7*}

1 Brain Science Institute, Johns Hopkins University School of Medicine, Baltimore, MD, 21205, United States of America, **2** Department of Neurology, Johns Hopkins University School of Medicine, Baltimore, MD, 21205, United States of America, **3** Next Generation Systems CFU, Eisai Inc., Andover, MA, 01810, United States of America, **4** Neuroscience and General Medicine PCU, Eisai Inc., Andover, MA, 01810, United States of America, **5** Department of Comparative Medicine and Molecular Pathobiology, Johns Hopkins University School of Medicine, Baltimore, MD, 21205, United States of America, **6** Department of Psychiatry, Johns Hopkins University School of Medicine, Baltimore, MD, 21205, United States of America, **7** Department of Neuroscience, Johns Hopkins University School of Medicine, Baltimore, MD, 21205, United States of America

* crojas2@jhmi.edu (CR); bslusher@jhmi.edu (BSS)



OPEN ACCESS

Citation: Thomas AG, Sattler R, Tendyke K, Loiacono KA, Hansen H, Sahni V, et al. (2015) High-Throughput Assay Development for Cystine-Glutamate Antiporter (x_c^-) Highlights Faster Cystine Uptake than Glutamate Release in Glioma Cells. PLoS ONE 10(8): e0127785. doi:10.1371/journal.pone.0127785

Editor: Hendrik W. van Veen, University of Cambridge, UNITED KINGDOM

Received: June 9, 2014

Accepted: April 19, 2015

Published: August 7, 2015

Copyright: © 2015 Thomas et al. This is an open access article distributed under the terms of the [Creative Commons Attribution License](https://creativecommons.org/licenses/by/4.0/), which permits unrestricted use, distribution, and reproduction in any medium, provided the original author and source are credited.

Data Availability Statement: All relevant data are within the paper and its Supporting Information files.

Funding: This work was supported through the NIH R21NS074062A1 and the 2P30 MH075673-06 grants awarded to BSS. Eisai Inc., provided support in the form of salaries for authors KT, KAL, HH, VS, and YH. The funders had no role in study design, data collection and analysis, decision to publish, or preparation of the manuscript. The specific roles of the authors are listed in the authors contributions section.

Abstract

The cystine-glutamate antiporter (system x_c^-) is a Na^+ -independent amino acid transporter that exchanges extracellular cystine for intracellular glutamate. It is thought to play a critical role in cellular redox processes through regulation of intracellular glutathione synthesis via cystine uptake. In gliomas, system x_c^- expression is universally up-regulated while that of glutamate transporters down-regulated, leading to a progressive accumulation of extracellular glutamate and excitotoxic cell death of the surrounding non-tumorous tissue. Additionally, up-regulation of system x_c^- in activated microglia has been implicated in the pathogenesis of several neurodegenerative disorders mediated by excess glutamate. Consequently, system x_c^- is a new drug target for brain cancer and neuroinflammatory diseases associated with excess extracellular glutamate. Unfortunately no potent and selective small molecule system x_c^- inhibitors exist and to our knowledge, no high throughput screening (HTS) assay has been developed to identify new scaffolds for inhibitor design. To develop such an assay, various neuronal and non-neuronal human cells were evaluated as sources of system x_c^- . Human glioma cells were chosen based on their high system x_c^- activity. Using these cells, [^{14}C]-cystine uptake and cystine-induced glutamate release assays were characterized and optimized with respect to cystine and protein concentrations and time of incubation. A pilot screen of the LOPAC/NINDS libraries using glutamate release demonstrated that the logistics of the assay were in place but unfortunately, did not yield meaningful pharmacophores. A larger, HTS campaign using the 384-well cystine-induced glutamate release as primary assay and the 96-well ^{14}C -cystine uptake as confirmatory assay is currently underway. Unexpectedly, we observed that the rate of cystine

Competing Interests: KT, KAL, HH, VS, and YH are employees of Eisai, Inc. There are no patents, products in development or marketed products to declare. This does not alter the authors' adherence to PLOS ONE policies on sharing data and materials.

uptake was significantly faster than the rate of glutamate release in human glioma cells. This was in contrast to the same rates of cystine uptake and glutamate release previously reported in normal human fibroblast cells.

Introduction

The cystine-glutamate antiporter (system x_c^-) is a Na^+ -independent amino acid transporter that exchanges extracellular cystine for intracellular glutamate [1]. Since cystine is a precursor for glutathione (GSH), system x_c^- is believed to play a critical role in intracellular GSH synthesis and subsequent cellular redox regulation [2]. Additionally, the release of glutamate into the extracellular space, via the antiporter, makes system x_c^- a key determinant of extracellular glutamate concentrations.

System x_c^- is thought to play a significant role in the pathogenesis of cancer and neurodegenerative diseases. In gliomas, system x_c^- expression is universally up-regulated and glutamate transporters are down-regulated, leading to a progressive accumulation of extracellular glutamate, thereby causing peritumoral seizures and excitotoxic cell death to surrounding neurons [3]. This provides a significant growth advantage to the tumor by offering space for expansion [4–7]. Additionally, glioma cells have a unique requirement for extracellular cystine, as they tend to lack the ability to synthesize cysteine [8]. This renders extracellular cystine uptake critical for glutathione synthesis and thus, tumor survival and growth [2, 9–11]. In fact, inhibitors of system x_c^- have been shown to significantly reduce brain tumor growth, block abnormal EEG and seizure activity, attenuate peritumoral edema and increase survival in animal models [9, 12].

Glutamate release has also been shown to be mediated via system x_c^- in activated microglia [13, 14]. Given the antiporter's potential involvement in glutamate excitotoxicity, up-regulation of system x_c^- in activated microglia has also been implicated in the pathogenesis of many neurodegenerative disorders [15], including Alzheimer's disease [16], Parkinson's disease [17], HIV-associated neurocognitive disorders [18], multiple sclerosis [19] and epilepsy [20].

Considering the potential role of system x_c^- in cancer and neurodegenerative diseases, as well as the validation of the target via both genetic (with siRNA) and pharmacological (with prototype small molecules) inhibition of the antiporter in pre-clinical models [9, 12], it is of interest to develop system x_c^- inhibitors that could be evaluated in the clinic. While a number of small molecule system x_c^- inhibitors has been described, none have shown potency and selectivity for the target [21–25]. Several prototype antiporter inhibitors are glutamate mimics, such as (S)-4-carboxyphenylglycine ((S)-4CPG), but they also have activity at various glutamate receptors and hence lack specificity [23, 24]. Sulfasalazine (SAS), a FDA approved drug for the treatment of Crohn's disease, is also an inhibitor of system x_c^- [26]. However, SAS lacks selectivity as it possesses both anti-inflammatory and antibacterial activity and inhibits NF- κ B [27]. SAS is also extensively metabolized *in vivo* by intestinal bacteria to 5-aminosalicylic acid and sulfapyridine, both metabolites being inactive against system x_c^- [26]. Therefore, to fully exploit the therapeutic potential of this target, it is critical to identify new structural entities that potently and selectively inhibit system x_c^- . To our knowledge, no high throughput screening (HTS) assay has been developed for this target. Various assays have been used to identify system x_c^- activity including cystine [1, 3, 28] or glutamate uptake [7, 24] and cystine-induced glutamate release [7, 24]. Here, we describe the characterization of both a cystine uptake assay and a cystine-induced glutamate release assay for implementation in HTS using

human astrocytoma cells. We also show that the rate of uptake of cystine mediated by system x_c^- is approximately 10 to 14-fold higher than the rate of glutamate release in human glioma cells, which is in contrast to previous studies performed in normal human fibroblast [29].

Materials and Methods

Reagents

Unless otherwise stated, all chemicals and glutamate dehydrogenase (GDH) were obtained from Sigma-Aldrich (Sigma, St. Louis, MO).

Cell lines

Daudi (lymphoblast), CCF-STTG-1 (astrocytoma), H4 (neuroglioma), IMR-90 (fibroblast), THP-1 (monocytes), U-87 MG (glioblastoma), obtained from American Type Culture Collection (ATCC, Manassas, VA) and P-493 B (lymphoma) cells, obtained from Dr. Chi Dang (Abramson Cancer Center, University of Pennsylvania, Philadelphia, PA; *Nature* **458**, 762–765, 2009), were examined for system x_c^- activity. The Daudi, P-493 B, CCF-STTG-1 and THP-1 cells were grown in RPMI-1640 media (ATCC: 30–2001) containing 10% fetal bovine serum (FBS, ATCC: 30–2020) and 1% Antibiotic-Antimycotic (Ab-Am; Life Technologies, Grand Island, NY: 15240062). Growth media for THP-1 cells also included 0.05 mM β -mercaptoethanol. U-87 MG cells were grown in Eagle's MEM (EMEM, ATCC: 30–2003) containing 20% FBS and 1% Ab-Am, while IMR-90 cells were grown in EMEM with 10% FBS and 1% Ab-Am. Finally, the H4 cells were grown in Ham's F-12 Nutrient Mix, GlutaMax supplement (Life Technologies: 31765035) with 10% FBS and 1% Ab-Am.

Quantitative Reverse Transcription-PCR

Total RNA was isolated from the various cells using the RNEasy Mini kit (Qiagen, Valencia, CA) and converted to cDNA using the High Capacity cDNA Reverse Transcription kit (Applied Biosystems, Foster city, CA). Quantitative PCR was completed using TaqMan pre-made gene-specific probes designed against the light chain subunit of system x_c^- , specifically xCT or SLC7A11 (the catalytic unit of system x_c^- , conjugated to FAM reporter dye; Applied Biosystems: 4331182) and against the endogenous control, 18S ribosomal RNA (conjugated to VIC reporter dye; Applied Biosystems: 4319413E). The relative abundance of xCT in the various cell lines was determined using the $2^{-\Delta\Delta CT}$ method [30, 31] and presented as a percent of the levels in the human astrocytoma (CCF-STTG-1) line.

[14 C]-Cystine uptake assay

Cystine uptake procedures were adapted from previously published reports [3]. Early characterization work was carried out in a 12-well format and the assay later adapted and characterized in the 96-well format. Briefly, CCF-STTG-1 cells were seeded at 0.04×10^6 cells per well in 0.2 ml growth media and grown to confluence. On the day of the experiment, cells were washed three times (100 μ l/well) with pre-warmed (37°C) chloride-dependent, sodium-independent, uptake buffer (UB, contents in mM: choline chloride 137.5, KCl 5.36, KH_2PO_4 0.77, MgSO_4 0.71, CaCl_2 1.1, Glucose 10 and HEPES 10, pH 7.4) and the kinetics of uptake initiated upon the addition of L-[3,3'- 14 C]-cystine (PerkinElmer, Waltham, MA: NEC845050UC) in buffer, at 37°C, containing 0–400 μ M cystine (5.631 μ Ci/ μ mol). After 15 min, uptake was terminated by three washes (115 μ l/well) with ice-cold UB. Cells were then lysed with 0.1 N NaOH (100 μ l/well) and the radioactivity in the cells measured using scintillant-coated 96-well plates (PerkinElmer: 6005630) and normalized to protein contents. The assay was further characterized for

the dependence of ^{14}C -cystine uptake on protein content (mg/ml) and the time and temperature of incubation. To determine IC_{50} values, CCF-STTG-1 cells were similarly seeded and grown to confluence. On day 3, transport was initiated upon the addition of pre-warmed (37°C) [^{14}C]-cystine $80\ \mu\text{M}$ ($5.631\ \mu\text{Ci}/\mu\text{mol}$) in Earle's Balanced Salt Solution (EBSS, Sigma: E3024, contents in mM: NaCl 116.4, NaHCO_3 26.2, NaH_2PO_4 1.02, KCl 5.36, MgSO_4 0.81, CaCl_2 1.8 and Glucose 5.56, pH 7.4) in the presence and absence of inhibitors. Uptake was terminated after 15 min with washes of ice-cold EBSS, the cells lysed with 0.1 N NaOH and radioactivity in cells measured as previously mentioned. The data were then normalized to the 'totals' (uptake at 37°C in the absence of inhibitor) and 'blanks' (either uptake at 37°C in the presence of 1 mM SAS (96-well format) or uptake at 0°C in the absence of inhibitor (12-well format)) and presented as percent inhibition. Identical protocols were followed for IC_{50} determinations using UB or phosphate buffered saline (PBS; contents in mM: [S1 Table](#)) with CCF-STTG-1, neuroglioma (H4) or fibroblast (IMR-90) cells. When using human glioblastoma cells (U-87 MG) as the source of the antiporter, cells were seeded at 0.06×10^6 cells per 96-well in 0.3 ml growth media. On day 2, cystine uptake was conducted in the presence and absence of inhibitors as described previously. At the end of the experiment, cells were lysed and the radioactivity in cells measured using scintillant-coated 96-well plates and normalized to protein contents.

Cystine-induced glutamate release assay

Early characterization of the cystine-induced glutamate release assay was carried out in the 96-well format and later adapted to the 384-well format. Briefly, CCF-STTG-1 cells were seeded at 0.04×10^6 cells per 96-well and grown to confluence. On Day 3, cells were washed with pre-warmed (37°C) EBSS and transport initiated upon the addition of 0–400 μM cystine in buffer at 37°C . Cells were maintained for 2h at 37°C in an incubator with 5% CO_2 . At the end of the incubation period, cystine-induced glutamate release was measured directly. The assay was further characterized for the dependence of cystine-induced glutamate release on protein content (mg/ml) and the time of incubation. For IC_{50} determinations, cells were also seeded at 0.04×10^6 cells per 96-well (in 0.2 ml growth media) and on Day 3, cells were washed with pre-warmed (37°C) EBSS and transport initiated upon the addition of 80 μM cystine in the presence and absence of inhibitors. Cells were maintained at 37°C in an incubator with 5% CO_2 and the glutamate released over a 2h period measured. Identical protocols were followed for IC_{50} determinations using UB or PBS with CCF-STTG-1, neuroglioma (H4) or fibroblast (IMR-90) cells. U-87 MG cells were seeded at 0.06×10^6 cells per 96-well (in 0.3 ml growth media) and tested on Day2. When running the assay in the 384-well format, CCF-STTG-1 cells were seeded at 0.01×10^6 cells per well (in 0.025 ml growth media) and grown to confluence. Upon reaching confluence (Day 3), cells were washed ($4 \times 50\ \mu\text{l}/\text{wash}$) with room temperature EBSS using either Beckman Coulter's (Biomek NX^{P}) or Tecan's (Freedom EVO150) liquid handling system and transport initiated upon the addition of 80 μM cystine (20 μl). Cells were maintained for 3h at 37°C in an incubator with 5% CO_2 . At the end of the incubation period, cystine-induced glutamate release was measured directly.

Glutamate measurement

Cystine-induced glutamate released from cells was measured by coupling the effluxed glutamate to either glutamate dehydrogenase (GDH) [32] or glutamate oxidase (GO) [33]. When using GDH (5 U/mL, Sigma: G7882), the reaction was carried out in the presence of nicotinamide adenine dinucleotide phosphate (NADP^+ , 500 μM) to catalyze the conversion of glutamate to α -ketoglutarate, ammonia and NADPH (ex 340, em 460). When using GO

(0.04 U/mL, US Biological, Swampscott, MA: G4001-01), the reaction was carried out in the presence of molecular oxygen and water, to catalyze the conversion of glutamate to α -keto-glutarate, ammonia and hydrogen peroxide. In turn, hydrogen peroxide was detected with Amplex UltraRed (50 μ M, Life Technologies: A36006), in a reaction catalyzed by horse radish peroxidase (HRP; 0.125 U/mL, Worthington Biochemical, Lakewood, NJ: LS006476), to produce highly fluorescent resorufin (ex 530, em 590). Both GDH and GO assays were conducted in Tris buffer (100 mM, pH 7.4) and rate of change of fluorescence (RFU/s) monitored using Molecular Device's Spectramax Gemini XPS fluorimeter.

Libraries for screening

Two libraries of compounds were used initially to confirm that the logistics of the cystine-induced glutamate release were in place. (i) The Library of Pharmacologically Active Compounds, LOPAC¹²⁸⁰, (Sigma: LO4100-1EA) comprising 1,280 bioactive small molecules and approved drugs from all major drug classes and (ii) the National Institute of Neurological Disorders and Stroke (NINDS) Custom Collection (MicroSource Discovery Systems, CT) comprising 1,040 compounds, mostly FDA-approved and marketed drugs. Test compounds were made up in 100% DMSO and diluted 500-fold to minimize DMSO exposure on cells to 0.2%. Also, both 'blanks' (buffer) and 'totals' (buffer containing cystine 80 μ M) contained 0.2% DMSO to compensate for DMSO-solubilized compounds. Data were normalized to the totals and blanks and IC_{50} values determined as a function of the normalized values. Finally, since cystine-induced glutamate release assay uses GO and HRP for glutamate detection, compounds being evaluated for inhibition of system x_c^- activity could give false positive results as a consequence of inhibiting one of the two coupling enzymes. In order to rule out inhibition of the coupling enzymes, a counter screen was carried out in the absence of cells (the source of system x_c^-) but in the presence of both cystine and glutamate.

Data analysis

The K_m values were determined using GraphPad Prism employing least-squares fit of the Michaelis-Menten equation: $v = V_{max}[S]/(K_m + [S])$. Lineweaver-Burk plots were used to illustrate results from the least-squares fit. The half maximal inhibitory constant (IC_{50}) was also determined using GraphPad Prism. Data were normalized to the 'totals' (maximum transport or glutamate release) and 'blanks' (minimum transport or glutamate release) and IC_{50} values calculated as a function of the normalized values.

Results

System x_c^- expression and activity is highest in glioma cells

Assessment of the mRNA expression of the catalytic subunit of system x_c^- ($xCT/SLC7A11$) with the cystine-induced glutamate release activity (see below; expressed here as RFU/s per mg protein) in various non-neuronal, non-adherent human cells (Daudi, P-493 B, THP-1), non-neuronal, adherent human cells (IMR-90) and neuronal, adherent human cells (CCF-STTG-1, H4, U-87 MG) showed a correlation coefficient of 0.96 between $SLC7A11$ mRNA levels and activity (Table 1). The highest mRNA and functional transport activity levels were found in the human, neuronal lines, specifically in the neuroglioma (H4) and the grade IV astrocytoma (CCF-STTG-1) cells. Further characterization studies were carried out using these adherent astrocytoma (CCF-STTG-1) cells.

Table 1. $xCT/SLC7A11$ mRNA and cystine-induced glutamate release activity in various cell lines.

Cell line	$xCT/SLC7A11$ mRNA (relative to CCF-STTG-1 cells)	System x_c^- activity (RFU. $s^{-1}.mg^{-1}$)
H4 (human neuroglioma)	172.55	13.76
CCF-STTG-1 (human astrocytoma)	100.00	6.20
IMR-90 (human fibroblast)	17.90	3.40
THP-1 (human monocytes)	8.85	1.31
DAUDI (human lymphoblast)	4.31	3.49
P-493 B (human lymphoma)	3.82	1.34
U-87 MG (human glioblastoma)	1.23	0.31

doi:10.1371/journal.pone.0127785.t001

[^{14}C]-Cystine uptake is dependent on cystine and protein concentrations and time of incubation

Substrate dependence using CCF-STTG-1 cells was initiated upon the addition of 0–400 μM L-[^{14}C]-cystine. The uptake of cystine through system x_c^- was linear at lower cystine concentrations and leveled off at the higher cystine concentrations, an indicator of transporter saturation (Fig 1A). Non-linear analysis for the apparent K_m yielded a concentration of $63 \pm 4 \mu M$, illustrated by the Lineweaver-Burk transformation (Fig 1B). The uptake of cystine was linear with respect to protein (mg/ml, Fig 1C) and time of incubation (Fig 1D). Additionally, cystine uptake was sensitive to the temperature of incubation, with no transport at 0°C and with increased uptake occurring at higher temperatures (Fig 1E).

Cystine-induced glutamate release is dependent on cystine and protein concentrations and time of incubation

Glutamate measurement. Glutamate efflux from CCF-STTG-1 cells as measured by GDH (S1A Fig) and GO (S1B Fig) resulted in similar IC_{50} values but with significantly improved specific rates (difference between ‘blanks’ (buffer) and ‘totals’ (buffer with cystine)) and Z' values when using GO based assay (S1B Fig). Subsequent glutamate release assays were conducted with glutamate metabolism coupled to GO.

Assay characterization. Substrate dependence in CCF-STTG-1 cells was initiated upon the addition of 0–400 μM cystine. Cystine-induced glutamate release through system x_c^- exhibited Michaelis-Menten behavior: glutamate release was linear at lower cystine concentrations and leveled off at the higher cystine concentrations (Fig 2A) with an apparent K_m of $84 \pm 12 \mu M$ and illustrated by the Lineweaver-Burk plot (Fig 2B). Cystine-induced glutamate release was linear up to a plating density of 60,000 cells/well (0.320 mg/ml; Fig 2C) and to an incubation time of 240 min (Fig 2D). Finally, optimization of glutamate-release assays in the 384-well format resulted in Z' values ranging from 0.5–0.7 across both different sections of the plate and the entire plate (Fig 3).

Cystine-induced glutamate release assay was used to screen the LOPAC and NINDS chemical libraries

An initial activity analysis using ‘totals’ (buffer containing cystine 80 μM), with and without 0.2% DMSO, gave similar rates of change of fluorescence (S2 Table). Consequently, test compounds were made up at 500X the final concentration in 100% DMSO to limit DMSO exposure on cells to 0.2%. Compounds in the LOPAC and NINDS libraries were evaluated for

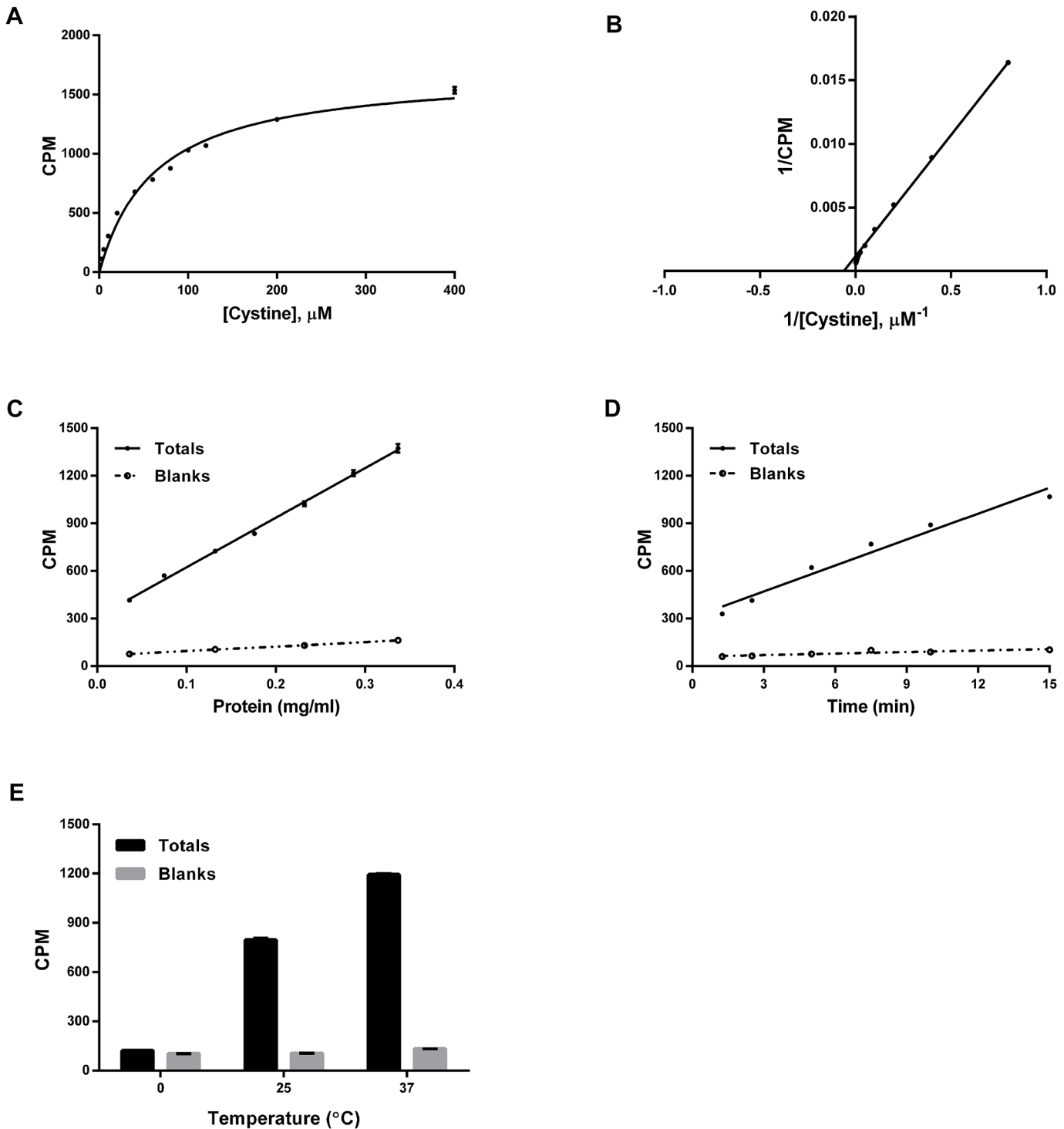


Fig 1. Dependence of [¹⁴C]-cystine uptake in CCF-STTG-1 cells on A. cystine concentration, B. cystine concentration represented via Lineweaver-Burk transformation, C. protein concentration (mg/ml), D. time and E. temperature of incubation. Unless otherwise specified, CCF-STTG-1 cells were seeded at 0.04×10^6 cells per 96-well, grown to confluence (Day 3), washed with pre-warmed chloride-dependent, sodium-independent, uptake buffer and transport initiated upon the addition of L-[3,3'-¹⁴C]-cystine at a specific activity of 5.631 $\mu\text{Ci}/\mu\text{mol}$. Substrate dependence experiments were carried out with 0–400 μM cystine while protein-, time- and temperature-dependence experiments were carried out with 80 μM cystine. Except for the time-dependence experiments, uptake was terminated after 15 min with washes of ice-cold uptake buffer. Subsequently, cells were lysed with 0.1 N NaOH and the radioactivity in the cells measured using a liquid scintillation counter and normalized to the protein contents. Data are an average of 2 or more independent experiments with 16–24 determinations per experiment.

doi:10.1371/journal.pone.0127785.g001

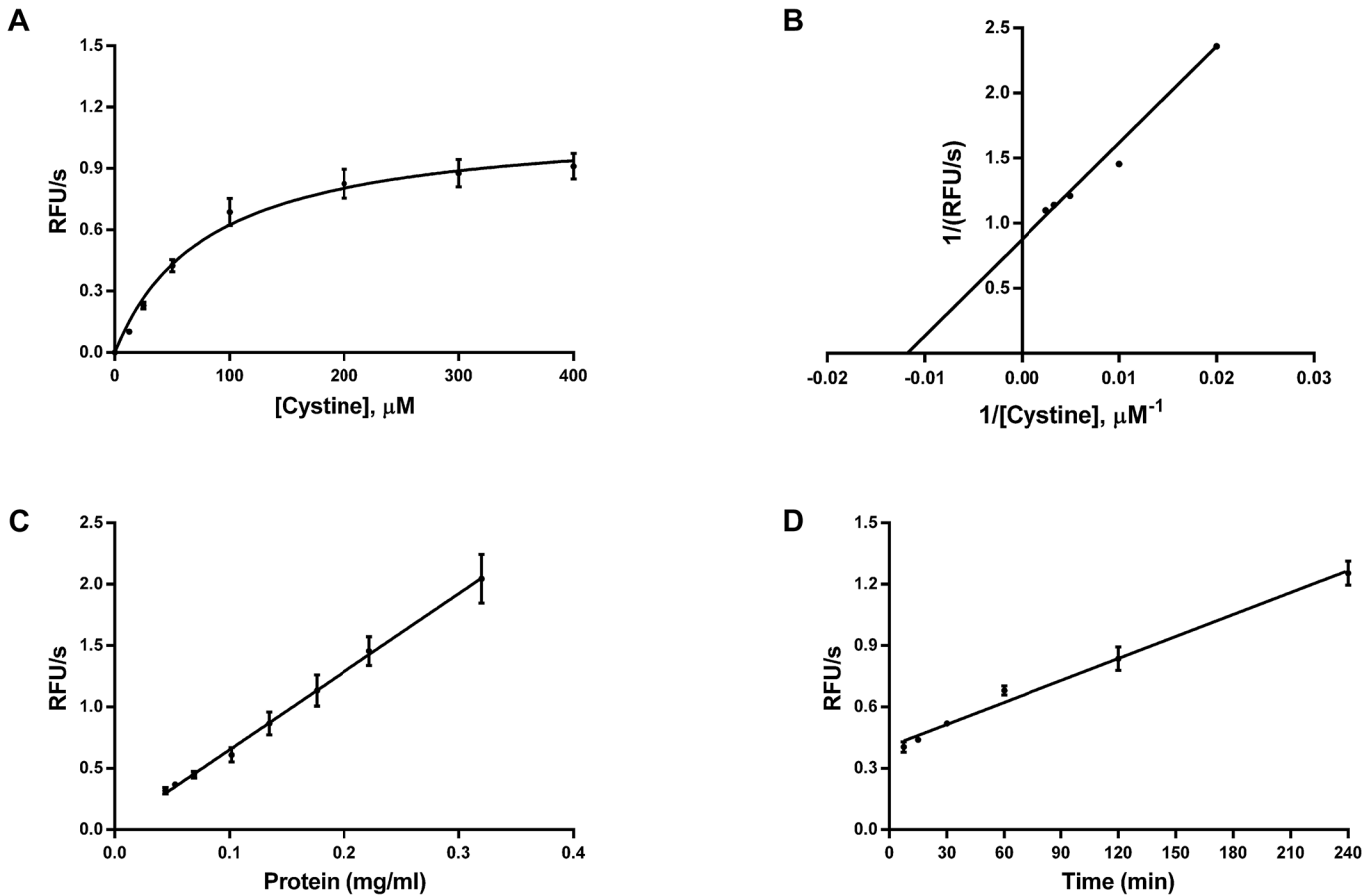


Fig 2. Dependence of cystine-induced glutamate release in CCF-STTG-1 cells at 37°C on A. cystine concentration, B. cystine concentration represented via Lineweaver-Burk transformation C. protein concentration (mg/ml) and D. time of incubation. Unless otherwise specified, CCF-STTG-1 cells were seeded at 0.04×10^6 cells per 96-well, grown to confluence (Day 3), washed with pre-warmed EBSS and transport initiated upon the addition of cystine. Substrate dependence experiments were carried out with 0–400 μM cystine while protein- and time-dependence experiments were carried out with 80 μM cystine. Cells were maintained for 2h at 37°C in an incubator with 5% CO_2 . At the end of the incubation period, glutamate release was measured directly using glutamate oxidase (0.04 U/mL), HRP (0.125 U/mL) and Amplex UltraRed (50 μM), in Tris buffer (100 mM, pH 7.4), at ex 530, em 590. Data are an average of 3 independent experiments with 16–24 determinations per experiment.

doi:10.1371/journal.pone.0127785.g002

system x_c^- activity at an initial concentration of 20 μM using the cystine-induced glutamate release assay. Out of 2320 compounds, 35 inhibited system x_c^- activity by 50% or higher. After excluding compounds that were auto fluorescent and fluorescence quenchers, a counter screen was carried out to detect inhibitors of either glutamate oxidase or HRP. The hits are shown in Fig 4.

IC₅₀ values in cystine-induced glutamate release assays are lower than those in cystine uptake assays within each cell line

Known inhibitors of system x_c^- , SAS and (S)-4CPG, were evaluated in both assays using CCF-STTG-1 cells as the source of the antiporter. Selectivity was verified with the known inactive enantiomer, (R)-4CPG. While both SAS and (S)-4CPG inhibited cystine transport and cystine-induced glutamate release through system x_c^- , (R)-4CPG did not (Table 2, Fig 5). The IC₅₀ values for inhibition of glutamate release were lower than the IC₅₀ values for inhibition of cystine uptake within each cell line (Table 2). On the other hand, the IC₅₀ values of (S)-4CPG, (R)-4CPG, SAS and the co-transporter, glutamate (in the uptake assay), were similar across

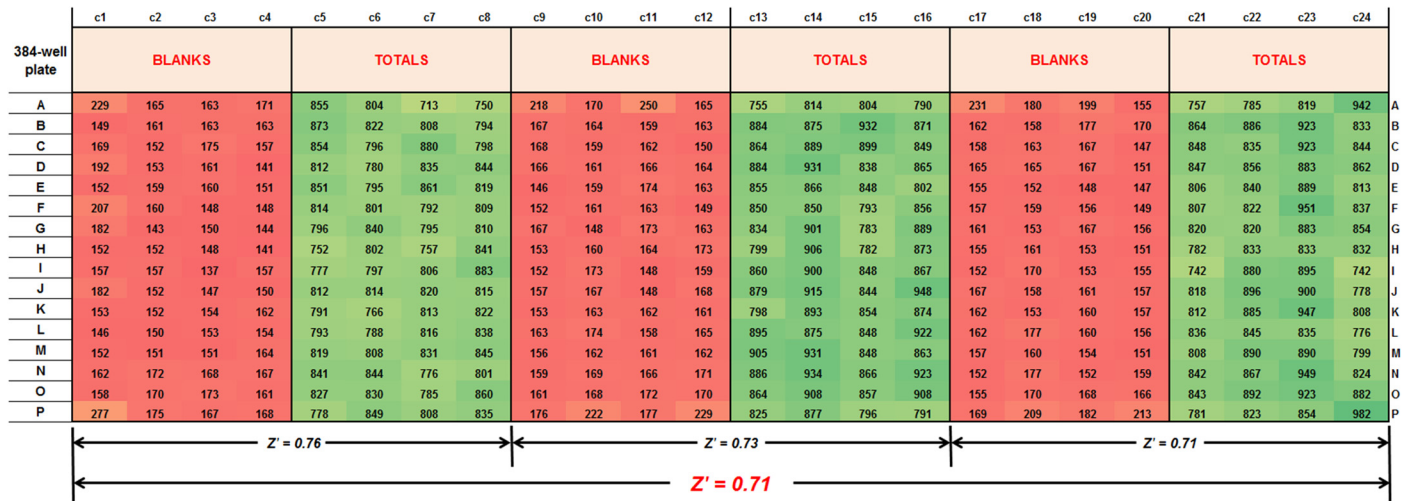


Fig 3. Heat map of 384-well cystine-induced glutamate release assay variability post-optimization. Uniformity in color, for both blanks and totals, illustrates the Z' values. CCF-STTG-1 cells were seeded at 0.01 x 10⁶ cells per 384-well in 0.025 ml growth media and grown to confluence. On Day 3, cells were washed (4 x 50 µl/wash) with EBSS (at RT) using either Beckman Coulter's (Biomek NX^P) or Tecan's (Freedom EVO150) liquid handling systems and transport initiated upon the addition of 80 µM cystine (20 µl). Cystine-induced glutamate release after 3h at 37°C was measured upon the addition of 25 µl of glutamate oxidase (0.04 U/mL), HRP (0.125 U/mL) and Amplex UltraRed (50 µM) in Tris buffer (100 mM, pH 7.4) and fluorescence followed at ex 530, em 590.

doi:10.1371/journal.pone.0127785.g003

Compound ID	Molecular Structure	MW	clog P	Average IC ₅₀ (µM)
L-798106 EP3-selective antagonist		536	6.389	20
TTNPB Selective and highly potent retinoic acid analog		348	6.919	20
CANDESARTAN CILEXTIL angiotensin 1 receptor antagonist		611	6.895	10

Fig 4. Initial screening results of the compounds in the LOPAC and NINDS chemical libraries using the cystine-induced glutamate release assay. CCF-STTG-1 cells were seeded and grown to confluence. On Day 3, cells were washed with pre-warmed EBSS and transport initiated upon the addition of cystine (80 µM). Cystine-induced glutamate released over 2h at 37°C, in the presence and absence of inhibitors, was measured directly using glutamate oxidase, horse radish peroxidase and Amplex UltraRed and the rate of change of fluorescence monitored at ex 530, em 590. Results were normalized to totals and blanks and the IC₅₀ values determined as a function of the normalized values.

doi:10.1371/journal.pone.0127785.g004

Table 2. IC₅₀ values (μM) of (S)-, (R)-4CPG, glutamate and sulfasalazine (SAS) in [¹⁴C]-cystine uptake and cystine-induced glutamate release assays using different cell sources of the antiporter and under different buffering conditions. Cystine uptake and glutamate release assays were carried out within the linear range for both processes; 15 min and 2 h, respectively.

UB (-Na ⁺)							
Lines tested	Cystine Uptake			Glutamate Release			SAS
	(S)-4CPG	(R)-4CPG	Glutamate	(S)-4CPG	(R)-4CPG	SAS	
CCF-STTG-1	10 ± 0.6	> 500	600 ± 30	40 ± 1	2 ± 0.4	> 100	20 ± 0.7
U-87 MG*	20 ± 1	> 1000	300 ± 10	30 ± 2	-	-	-
IMR-90*	30 ± 1	> 500	200 ± 9	40 ± 2	-	-	-
H4	20 ± 0.4	> 500	600 ± 20	40 ± 1	5 ± 0.7	> 100	30 ± 0.6
EBSS (+Na ⁺)							
Lines tested	Cystine Uptake			Glutamate Release			SAS
	(S)-4CPG	(R)-4CPG	Glutamate	(S)-4CPG	(R)-4CPG	SAS	
CCF-STTG-1	20 ± 0.9	> 500	500 ± 30	40 ± 3	2 ± 0.05	> 100	20 ± 0.5
U-87 MG	20 ± 1	> 500	200 ± 10	30 ± 1	3 ± 0.4	> 100	20 ± 0.4
IMR-90	50 ± 2	> 500	300 ± 30	50 ± 2	5 ± 0.7	> 100	5 ± 0.4
H4	20 ± 2	> 500	500 ± 10	40 ± 1	8 ± 1.0	> 100	20 ± 0.3

* No cystine-induced glutamate release in these lines under sodium-free conditions.

doi:10.1371/journal.pone.0127785.t002

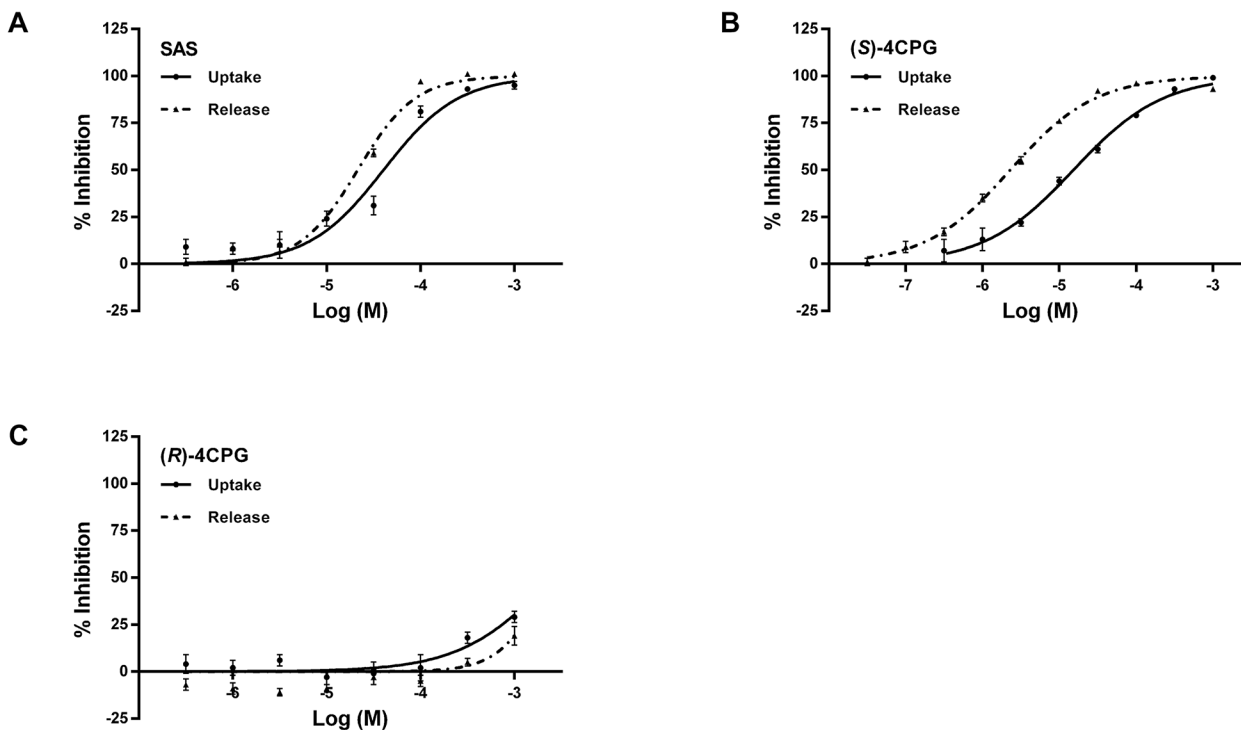


Fig 5. Dose responses of A. sulfasalazine (SAS), B. (S)-4-carboxyphenylglycine ((S)-4CPG) and C. (R)-4-carboxyphenylglycine ((R)-4CPG) using [¹⁴C]-cystine uptake and cystine-induced glutamate release assays in CCF-STTG-1 cells. Cystine uptake was conducted at 37°C for 15 min using 80 μM cystine, and at a specific activity of 5.631 μCi/μmol, in the presence and absence of inhibitors. At the end of the experiment, cells were lysed and the radioactivity in the cells measured using a scintillation counter and normalized to the protein contents. Cystine-induced glutamate released over 2h at 37°C upon the addition of 80 μM cystine, in the presence and absence of inhibitors, was measured directly using glutamate oxidase, horse radish peroxidase and Amplex UltraRed and the rate of change of fluorescence monitored at ex 530, em 590. For both assays, results were normalized to totals and blanks and the IC₅₀ values determined as a function of the normalized values. Data are an average of 2–6 independent experiments.

doi:10.1371/journal.pone.0127785.g005

multiple cell lines (CCF-STTG-1, U-87 MG, IMR-90, H4) regardless of the stoichiometry of cystine uptake to glutamate efflux (Tables 1 and 2). Furthermore, the IC_{50} values of SAS and (S)-4CPG were the same in the presence or absence of sodium (Table 2) or in a nominally, calcium-free buffer (no added calcium, formulation: S1 Table; data: S3 Table). Previously published analogs of SAS [25] were also evaluated in the release assay using CCF-STTG-1 cells as the source of system x_c^- . These yielded IC_{50} values comparable to the published reports, with similar rank order of potencies within the same chemical series (S4 Table).]

Comparison of the rate of cystine influx vs. the rate of glutamate efflux shows faster rate of cystine influx in glioma cells

The rates of [^{14}C]-cystine influx and cystine-induced glutamate efflux were closely examined using CCF-STTG-1 (grade IV astrocytoma) cells in order to understand the reasons for the lower IC_{50} values and longer time-dependence in the cystine-induced glutamate release assay. Cells were seeded similarly (40,000 cells/well) and both experiments initiated (on Day 3) upon the addition of the same concentration of cystine (80 μM) under similar experimental conditions as published originally [29]. The experiments were repeated also using IMR-90 fibroblast cells derived from normal embryonic lung and a second cancer line, the H4 neuroglioma cells. IMR-90 cells showed a trend towards faster cystine uptake versus glutamate release but the difference was not significant (Fig 6A). In contrast, both CCF-STTG-1 and H4 cancer cells showed a statistically significant, 10 to 14-fold difference between the cystine uptake and cystine-induced glutamate efflux rates.

Discussion

System x_c^- is a promising therapeutic target due to its ability to play a critical role in cancer therapy, via modulation of both glutathione biosynthesis and glutamate release, and in neurodegenerative diseases via regulation of extracellular glutamate. However, system x_c^- has received little attention partly due to the potential safety risk associated with blocking glutathione biosynthesis and partly due to the lack of selective and potent small molecule system x_c^- inhibitors. Indeed, while some cell-based studies indicate that loss of system x_c^- function leads to cytotoxic effects [34, 35], two different strains of mice lacking system x_c^- function have been reported to be healthy in appearance and fertile [36, 37]. Furthermore, siRNAs against system x_c^- have not shown any major side effects [12]. Here, as a first step to identify new scaffolds for inhibitor design, we developed a high throughput screening assay against system x_c^- . We report on the characterization and implementation of a [^{14}C]-cystine uptake assay and a cystine-induced glutamate release assay.

Various transport assays used to identify system x_c^- activity have included [3H]-cystine [1], [^{14}C]-cystine [28], [^{35}S]-cystine [3], [3H]-glutamate uptake assays [7, 24] as well as cystine-induced glutamate release assays [7, 24, 29]. However, since [^{35}S] has a relatively short half-life of 87 days [38], [3H]-cystine is no longer commercially available and the physiological flux via system x_c^- involves the entry of L-cystine and the exit of L-glutamate [28], [^{35}S]-, [3H]-cystine and [3H]-glutamate uptake assays were not considered as viable options. Instead, a direct, [^{14}C]-cystine uptake assay [28] and a cystine-induced glutamate release assay [7, 24, 29] were used to define system x_c^- activity.

A second key determinant in the characterization of the assay was the source of system x_c^- . The best cell source of the transporter was determined based on system x_c^- activity measured by cystine-induced glutamate release. Multiple non-neuronal, non-adherent and neuronal, adherent human cells were assessed for system x_c^- activity. The highest expression and activity levels were observed in the newly acquired human neuroglioma cells (H4) and the human

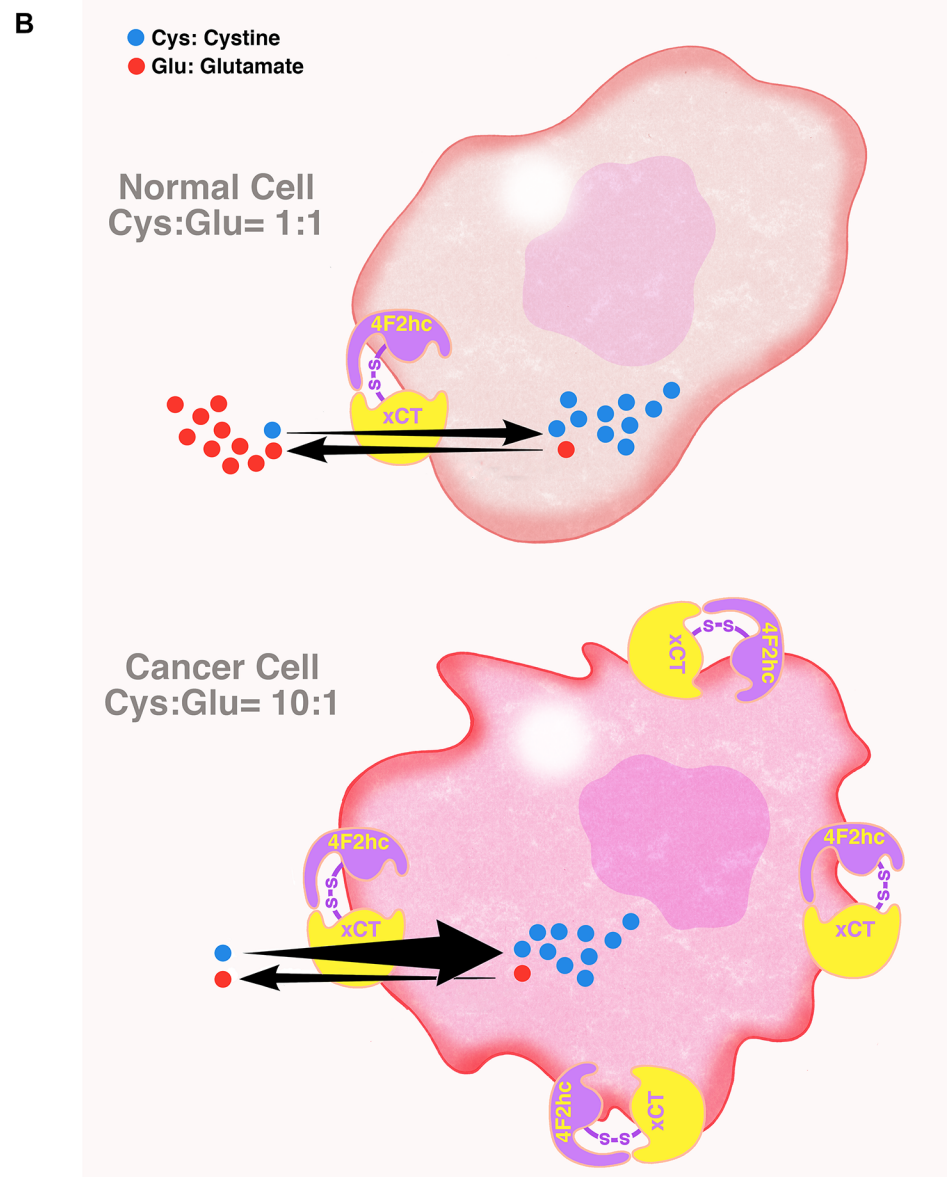
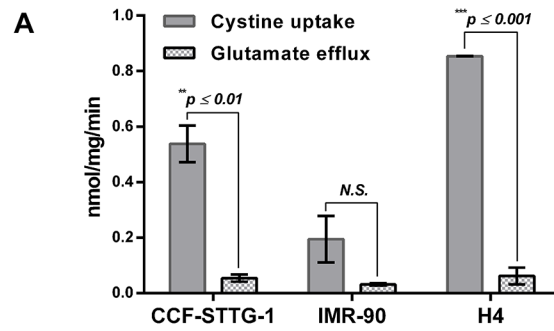


Fig 6. A. Rates of [14 C]-cystine influx and cystine-induced glutamate efflux in CCF-STTG-1, IMR-90 and H4 cells. Experiments were performed using previously published protocols [29] with minor modifications. Cells were seeded at 0.04×10^6 cells per 96-well, grown to confluence (Day 3), washed with pre-warmed PBS, and experiments initiated upon the addition of 80 μ M cystine with or without L-[3,3'- 14 C]-cystine (5.631 μ Ci/ μ mol). Cystine uptake was terminated after 2 min and cystine-induced glutamate release measured after 30 min.

The rates of cystine uptake and cystine-induced glutamate release were calculated from an average of 2 independent experiments with 16 determinations per experiment and normalized to time and protein content (nmol/mg/min \pm SD); ** $p < 0.001$ vs. rate of glutamate efflux; N.S.—not significant. B. Proposed schema for system x_c^- activity and glutamate metabolism in normal (top) and cancer cells (bottom). In both normal and cancer cells, the affinities (K_m) of system x_c^- for extracellular cystine and intracellular glutamate are 0.05 mM and 7.5 mM, respectively [29]. Normal cells exhibit a 1:1 ratio of cystine uptake to glutamate release. Cancer cells exhibit a ≥ 10 :1 ratio of cystine uptake to glutamate release.

doi:10.1371/journal.pone.0127785.g006

astrocytoma cells (CCF-STTG-1, Table 1). There was a strong correlation between $xCT/SLC7A11$ mRNA expression and transporter activity (0.96) suggesting that the control of gene expression occurred primarily at the level of transcription rather than at the level of translation.

System x_c^- activity, as defined by [^{14}C]-cystine uptake using CCF-STTG-1 cells, followed Michaelis-Menten kinetics, with apparent K_m consistent with earlier reports [1, 3, 28], and exhibited protein-, time- and temperature-dependence (Fig 1). Uptake was linear up to 15 min (time course at 37°C; Fig 1D) suggesting no immediate egress of the label from the cells. However, at longer incubations (> 15 min), [^{14}C]-cystine uptake resulted in lower specific rates (data not shown), consistent with [^{14}C]-efflux out of cells via cysteine formation [3, 39]. Known inhibitors of system x_c^- [24, 26] gave similar IC_{50} values as those reported previously [9, 40] (Table 2, Fig 5) corroborating earlier reports of Na^+ -independent L-cystine uptake [3, 28]. The co-transporter, glutamate, also inhibited cystine uptake with comparable inhibitory potency across all cell types (IC_{50} : 200–600 μM ; Table 2) irrespective of sodium. Additionally, using previously published protocols [1], the IC_{50} for glutamate was also consistent with its reported K_i against cystine uptake (in IMR-90 cells, S5 Table). However, as a HTS assay, the uptake assay is limited in its scope by (i) the sensitivity of the transport to temperature of the wash and assay buffers (Fig 1E), (ii) the necessity for multiple washes before and after transport, (iii) the need for transfer of cell lysate to a solid scintillator plate and (iv) the cost of the label. Consequently, it was decided that [^{14}C]-cystine uptake assay would be most useful in a HTS campaign as a confirmatory assay rather than as a primary screening assay.

An alternative way to assess system x_c^- activity was to measure cystine-induced glutamate release [7, 24, 29]. System x_c^- activity as measured by the coupling of the glutamate efflux via the transporter to its extracellular metabolism by GO [33] provided greater sensitivity and most importantly, direct, online measurement capabilities (i.e., cystine-induced glutamate release and its detection made in the same well) than previously described glutamate analysis [29] or GDH mediated methods [7, 24] (S1 Fig). Cystine-induced glutamate release through system x_c^- also exhibited Michaelis-Menten behavior (Fig 2A) with apparent K_m similar to that obtained using the [^{14}C]-cystine uptake assay and comparable to those reported previously [3, 29]. This is not surprising since, in each case, the binding affinity (K_m) that is measured is the affinity of the transporter for cystine regardless of the different end point measurements. At 37°C, cystine-induced glutamate release also exhibited protein- and time-dependence (Fig 2). Interestingly, glutamate release was linear over a 4h period (Fig 2D), and potentially longer [3], in contrast to the time-dependence data for cystine uptake (Fig 1D). This disparity could be due to the time taken by intercellular glutamate precursors to generate and subsequently release glutamate [3]. For the 384-well assay, additional optimization in terms of wash buffer temperature, number of washes, wash volumes, aspiration and dispense speeds resulted in minimal assay variability between different sections of the plate and across the entire plate (Z' values of 0.5–0.7; Fig 3). Final assay characterization using known inhibitors of system x_c^- [24, 26], in Na^+ -free and Na^+ -containing buffers, resulted in similar IC_{50} values (Table 2). Also, the

absence of calcium did not alter the IC_{50} values of the prototypes (S2 Table). Additionally, a pilot screen of the LOPAC and the NINDS libraries demonstrated that the logistics of the assay were in place. Unfortunately, the hit compounds were not amenable to medicinal chemistry optimization. In addition to being weak inhibitors of system x_c^- , the compounds exhibited low solubility ($\text{clog } P > 5$), had high molecular weights (except compound TTNPB), or were expected to have poor blood brain barrier penetrability (Fig 4).

Further validation with previously published SAS analogs [25] yielded comparable values and similar rank order of potency in both the glutamate release and uptake assays (S4 Table). Of note, were the relatively lower IC_{50} values of most compounds in the glutamate release assays as compared to the uptake assays (Tables 2 and S4, Fig 5). One plausible explanation is that cystine uptake may be mediated through other routes of entry besides system x_c^- [41]. That cystine uptake occurs without concomitant glutamate release in both the U-87 MG human glioblastoma cells and in the IMR-90 human fibroblast cells in the absence of sodium (Table 2) suggests a different pathway for cystine ingress. An alternative, though not mutually exclusive, explanation for the discrepancy in IC_{50} values between the two assays is that, in the glutamate release assay, a system x_c^- inhibitor could be blocking both the influx of cystine and the subsequent cystine-induced efflux of glutamate, resulting in the appearance of a more potent system x_c^- inhibitor (lower IC_{50} value); whereas in the uptake assay, the IC_{50} values are reflective of only the direct blockage of [^{14}C]-cystine influx via the antiporter.

A closer look at the two assays for system x_c^- activity measurement revealed that, in CCF-STTG-1 cells, the rate of entry of cystine was more than 10-fold higher than the rate of exodus of glutamate (Fig 6A). Careful scrutiny of an earlier work with CCF-STTG-1 cells shows saturation of cystine uptake occurs within 20 min while cystine-induced glutamate release continues to occur even at 14 h [3] suggesting a faster cystine uptake rate than the glutamate efflux rate in accordance with our results. However, these results are in contrast to the 1:1 ratio reported previously for human fibroblast cells derived from normal embryonic lung (IMR-90 cells) [29]. A repeat of the experiments under originally published conditions [29], i.e. uptake at 2 min and release at 30 min, revealed a similar trend in normal IMR-90 cells as with glioma cells (Fig 6A). However, there was no significant difference between the two rates, in agreement with Bannai's earlier results [29]. In contrast, both the CCF-STTG-1 and H4 cancer cells showed a statistically significant, 10 to 14-fold higher cystine uptake to glutamate efflux rate. These results are consistent with the notion that glioma cells have a unique requirement for extracellular cystine for intracellular cysteine synthesis [8]. Furthermore, whereas the affinity (K_m) of system x_c^- for extracellular cystine is 0.05 mM, the affinity of the same transporter for intracellular glutamate is 7.5 mM [29]. While it is reasonable to assume that the affinities (K_m) of extracellular cystine and intracellular glutamate for the transporter is similar across different cell types, the amount of intracellular glutamate available for cystine-induced release may also be different due to the distinct metabolic needs of normal and cancer cells (Fig 6B). Recent evidence suggests that, in cancer cells, glutamate maybe re-routed as an oxidative substrate for the Krebs (tricarboxylic acid (TCA)) cycle to produce ATP [42–45], resulting in reduced glutamate availability for release. Since the affinity of intracellular glutamate for the transporter is much lower than that of extracellular cystine for the same transporter, much less glutamate gets out resulting in lower than expected rate of glutamate efflux. The lower IC_{50} values in the glutamate release assays are consistent with also this hypothesis.

Regardless of the differences in IC_{50} values, these assays that have been characterized are designed to identify inhibitors of system x_c^- that could impede cancer cell growth via disruption of GSH synthesis or prevent glutamate excitotoxicity in neurodegenerative diseases via interruption of microglial activation. Even though in these assays we follow cystine uptake and glutamate release, processes associated with system x_c^- , it is important to note that these assays are

phenotypic and reflect many other activities of the cell. It is conceivable that compounds identified as inhibitors of system x_c^- may also have an impact at many other sites, including those known to block microglial activation such as inhibitors of glutaminase, nuclear factor κ B, mitogen-activated protein kinases [46] and metabotropic glutamate receptor (mGluR) ligands [47, 48]. In fact, recent evidence indicates that glutamate release through system x_c^- is coupled to NADPH oxidase in microglia [49], an enzyme complex that maybe inhibited by activating mGluR's [50].

In summary, system x_c^- activity as defined by both [14 C]-cystine uptake and cystine-induced glutamate release were successfully characterized. A close examination of the characterization data using glioma cells revealed significantly faster cystine uptake than glutamate release. The 384-well cystine-induced glutamate release assay, along with a counter screen, is effectively being implemented to carry out a HTS campaign to identify ideal system x_c^- inhibitors for brain cancer and other neurodegenerative diseases associated with excess extracellular glutamate.

Supporting Information

S1 Table. Buffer formulations.

(DOCX)

S2 Table. Effect of 0.2% DMSO on 'totals' (buffer containing cystine 80 μ M; units: RFU/s) from cystine-induced glutamate release experiments.

(DOCX)

S3 Table. Effect of calcium on specific rates and IC_{50} values of (S)-, (R)-4CPG and sulfasalazine (SAS) in cystine uptake assays.

(DOCX)

S4 Table. IC_{50} values of sulfasalazine (SAS) and its analogs in [14 C]-cystine uptake and cystine-induced glutamate release assays. Compounds arranged as per rank order in [14 C]-cystine uptake.

(DOCX)

S5 Table. IC_{50} values (μ M) of (S)-, (R)-4CPG, glutamate and sulfasalazine (SAS) in [14 C]-cystine uptake (2 min) and cystine-induced glutamate release (30 min) assays using CCF-STTG-1, IMR-90 and H4 cells as per previously published methods [29].

(DOCX)

S6 Table. Cystine influx and glutamate efflux rates (nmol/mg/min) in CCF-STTG-1, IMR-90 and H4 cells as per previously published methods [29].

(DOCX)

S1 Fig. Cystine-induced glutamate detection in glioma cells using either A. glutamate dehydrogenase (5 U/mL) and NADP⁺ (500 μ M) or B. glutamate oxidase (0.04 U/mL), HRP (0.125 U/mL) and Amplex UltraRed (50 μ M). In both instances, assays were conducted in Tris buffer (100 mM, pH 7.4) and the rate of change of fluorescence monitored: NADPH formation at ex 340, em 460 and resorufin formation at ex 530, em 590. Z' values, specific rates and IC_{50} values of (S)-4CPG and (R)-4CPG are shown in the insets.

(TIF)

S1 File. Data [Table 1](#).

(XLSX)

S2 File. Data [Table 2](#).

(XLSX)

- S3 File. Data [Fig 1A and 1B](#).**
(XLSX)
- S4 File. Data [Fig 1C](#).**
(XLSX)
- S5 File. Data [Fig 1D](#).**
(XLSX)
- S6 File. Data [Fig 1E](#).**
(XLSX)
- S7 File. Data [Fig 2A and 2B](#).**
(XLSX)
- S8 File. Data [Fig 2C](#).**
(XLSX)
- S9 File. Data [Fig 2D](#).**
(XLSX)
- S10 File. Data [Fig 3](#).**
(XLSX)
- S11 File. Data [Fig 4](#).**
(XLSX)
- S12 File. Data [Fig 5A](#).**
(PZF)
- S13 File. Data [Fig 5B](#).**
(PZF)
- S14 File. Data [Fig 5C](#).**
(PZF)
- S15 File. Data [Fig 6A](#), [S5 Table](#), [S6 Table](#)–Cystine uptake.**
(XLSX)
- S16 File. Data [Fig 6A](#), [S5 Table](#), [S6 Table](#)–Glutamate efflux.**
(XLSX)
- S17 File. Data [S2 Table](#).**
(XLSX)
- S18 File. Data [S3 Table](#).**
(XLSX)
- S19 File. Data [S4 Table](#).**
(XLSX)
- S20 File. Data [S5 Table](#).**
(XLSX)
- S21 File. Data [S1 Fig](#).**
(XLSX)

Acknowledgments

The authors wish to acknowledge the cell culture support provided by Alice Nunes, Irina Shats, Yoko Ayukawa and Benjamin N. Hoover from the Department of Neurology, Johns Hopkins University, Baltimore, MD 21205. We are also deeply grateful to Benjamin for assistance with the xCT mRNA probe design and analysis and to Sveta Vidensky for additional xCT mRNA analysis. We also wish to acknowledge the technical contributions made by Akihiko Koyama in the design of the 384-well assay at Neuroscience and General Medicine PCU, Eisai Inc., Andover, MA.

Author Contributions

Conceived and designed the experiments: AGT CR BSS. Performed the experiments: AGT RS KT KAL. Analyzed the data: AGT RS KT KAL. Contributed reagents/materials/analysis tools: AGT RS KT KAL HH VS YH CR BSS. Wrote the paper: AGT RS HH VS CR BSS.

References

1. Bannai S, Kitamura E. Transport interaction of L-cystine and L-glutamate in human diploid fibroblasts in culture. *J Biol Chem*. 1980; 255(6):2372–6. Epub 1980/03/25. PMID: [7358676](#).
2. Griffith OW. Biologic and pharmacologic regulation of mammalian glutathione synthesis. *Free Radic Biol Med*. 1999; 27(9–10):922–35. Epub 1999/11/24. doi: S0891-5849(99)00176-8 [pii]. PMID: [10569625](#).
3. Ye ZC, Rothstein JD, Sontheimer H. Compromised glutamate transport in human glioma cells: reduction-mislocalization of sodium-dependent glutamate transporters and enhanced activity of cystine-glutamate exchange. *J Neurosci*. 1999; 19(24):10767–77. Epub 1999/12/14. PMID: [10594060](#).
4. Lyons SA, Chung WJ, Weaver AK, Ogunrinu T, Sontheimer H. Autocrine glutamate signaling promotes glioma cell invasion. *Cancer Res*. 2007; 67(19):9463–71. Epub 2007/10/03. doi: 67/19/9463 [pii] doi: [10.1158/0008-5472.CAN-07-2034](#) PMID: [17909056](#); PubMed Central PMCID: PMC2045073.
5. Sontheimer H. Malignant gliomas: perverting glutamate and ion homeostasis for selective advantage. *Trends Neurosci*. 2003; 26(10):543–9. Epub 2003/10/03. doi: S0166-2236(03)00265-0 [pii] doi: [10.1016/j.tins.2003.08.007](#) PMID: [14522147](#).
6. Takano T, Lin JH, Arcuino G, Gao Q, Yang J, Nedergaard M. Glutamate release promotes growth of malignant gliomas. *Nat Med*. 2001; 7(9):1010–5. Epub 2001/09/05. doi: [10.1038/nm0901-1010](#) [pii]. PMID: [11533703](#).
7. Ye ZC, Sontheimer H. Glioma cells release excitotoxic concentrations of glutamate. *Cancer Res*. 1999; 59(17):4383–91. Epub 1999/09/15. PMID: [10485487](#).
8. Iglehart JK, York RM, Modest AP, Lazarus H, Livingston DM. Cystine requirement of continuous human lymphoid cell lines of normal and leukemic origin. *J Biol Chem*. 1977; 252(20):7184–91. Epub 1977/10/25. PMID: [903356](#).
9. Chung WJ, Lyons SA, Nelson GM, Hamza H, Gladson CL, Gillespie GY, et al. Inhibition of cystine uptake disrupts the growth of primary brain tumors. *J Neurosci*. 2005; 25(31):7101–10. Epub 2005/08/05. doi: 25/31/7101 [pii] doi: [10.1523/JNEUROSCI.5258-04.2005](#) PMID: [16079392](#); PubMed Central PMCID: PMC2681064.
10. Iida M, Sunaga S, Hirota N, Kuribayashi N, Sakagami H, Takeda M, et al. Effect of glutathione-modulating compounds on hydrogen-peroxide-induced cytotoxicity in human glioblastoma and glioma cell lines. *J Cancer Res Clin Oncol*. 1997; 123(11–12):619–22. Epub 1997/01/01. PMID: [9620220](#).
11. Mitchell JB, Cook JA, DeGraff W, Glatstein E, Russo A. Glutathione modulation in cancer treatment: will it work? *Int J Radiat Oncol Biol Phys*. 1989; 16(5):1289–95. Epub 1989/05/01. doi: 0360-3016(89)90301-5 [pii]. PMID: [2654105](#).
12. Savaskan NE, Heckel A, Hahnen E, Engelhorn T, Doerfler A, Ganslandt O, et al. Small interfering RNA-mediated xCT silencing in gliomas inhibits neurodegeneration and alleviates brain edema. *Nat Med*. 2008; 14(6):629–32. Epub 2008/05/13. doi: nm1772 [pii] doi: [10.1038/nm1772](#) PMID: [18469825](#).
13. Domercq M, Sanchez-Gomez MV, Sherwin C, Etxebarria E, Fern R, Matute C. System xc⁻ and glutamate transporter inhibition mediates microglial toxicity to oligodendrocytes. *J Immunol*. 2007; 178(10):6549–56. Epub 2007/05/04. doi: 178/10/6549 [pii]. PMID: [17475885](#).
14. Kigerl KA, Ankeny DP, Garg SK, Wei P, Guan Z, Lai W, et al. System x(c)⁻ regulates microglia and macrophage glutamate excitotoxicity in vivo. *Exp Neurol*. 2012; 233(1):333–41. Epub 2011/11/15. doi:

- S0014-4886(11)00397-9 [pii] doi: [10.1016/j.expneurol.2011.10.025](https://doi.org/10.1016/j.expneurol.2011.10.025) PMID: [22079587](https://pubmed.ncbi.nlm.nih.gov/22079587/); PubMed Central PMCID: [PMC3268895](https://pubmed.ncbi.nlm.nih.gov/PMC3268895/).
15. Albrecht P, Lewerenz J, Dittmer S, Noack R, Maher P, Methner A. Mechanisms of oxidative glutamate toxicity: the glutamate/cystine antiporter system x_c^- as a neuroprotective drug target. *CNS Neurol Disord Drug Targets*. 2010; 9(3):373–82. Epub 2010/01/08. doi: [BSP/CDTCNSND/E-Pub/00018](https://doi.org/BSP/CDTCNSND/E-Pub/00018) [pii]. PMID: [20053169](https://pubmed.ncbi.nlm.nih.gov/20053169/).
 16. Qin S, Colin C, Hinners I, Gervais A, Cheret C, Mallat M. System X_c^- and apolipoprotein E expressed by microglia have opposite effects on the neurotoxicity of amyloid-beta peptide 1–40. *J Neurosci*. 2006; 26(12):3345–56. Epub 2006/03/24. doi: [10.1523/JNEUROSCI.5186-05.2006](https://doi.org/10.1523/JNEUROSCI.5186-05.2006) [pii] doi: [10.1523/JNEUROSCI.5186-05.2006](https://doi.org/10.1523/JNEUROSCI.5186-05.2006) PMID: [16554485](https://pubmed.ncbi.nlm.nih.gov/16554485/).
 17. Massie A, Schallier A, Kim SW, Fernando R, Kobayashi S, Beck H, et al. Dopaminergic neurons of system $x(c)^-$ -deficient mice are highly protected against 6-hydroxydopamine-induced toxicity. *FASEB J*. 2011; 25(4):1359–69. Epub 2010/12/31. doi: [fj.10-177212](https://doi.org/fj.10-177212) [pii] doi: [10.1096/fj.10-177212](https://doi.org/10.1096/fj.10-177212) PMID: [21191088](https://pubmed.ncbi.nlm.nih.gov/21191088/).
 18. Gupta S, Knight AG, Knapp PE, Hauser KF, Keller JN, Bruce-Keller AJ. HIV-Tat elicits microglial glutamate release: role of NADPH oxidase and the cystine-glutamate antiporter. *Neurosci Lett*. 2010; 485(3):233–6. Epub 2010/09/21. doi: [S0304-3940\(10\)01210-3](https://doi.org/S0304-3940(10)01210-3) [pii] doi: [10.1016/j.neulet.2010.09.019](https://doi.org/10.1016/j.neulet.2010.09.019) PMID: [20849923](https://pubmed.ncbi.nlm.nih.gov/20849923/); PubMed Central PMCID: [PMC2956797](https://pubmed.ncbi.nlm.nih.gov/PMC2956797/).
 19. Pampliega O, Domercq M, Soria FN, Villoslada P, Rodriguez-Antiguedad A, Matute C. Increased expression of cystine/glutamate antiporter in multiple sclerosis. *J Neuroinflammation*. 2011; 8:63. Epub 2011/06/07. doi: [1742-2094-8-63](https://doi.org/1742-2094-8-63) [pii] doi: [10.1186/1742-2094-8-63](https://doi.org/10.1186/1742-2094-8-63) PMID: [21639880](https://pubmed.ncbi.nlm.nih.gov/21639880/); PubMed Central PMCID: [PMC3117706](https://pubmed.ncbi.nlm.nih.gov/PMC3117706/).
 20. De Bundel D, Schallier A, Loyens E, Fernando R, Miyashita H, Van Liefveringe J, et al. Loss of system $x(c)^-$ does not induce oxidative stress but decreases extracellular glutamate in hippocampus and influences spatial working memory and limbic seizure susceptibility. *J Neurosci*. 2011; 31(15):5792–803. Epub 2011/04/15. doi: [10.1523/JNEUROSCI.5465-10.2011](https://doi.org/10.1523/JNEUROSCI.5465-10.2011) [pii] doi: [10.1523/JNEUROSCI.5465-10.2011](https://doi.org/10.1523/JNEUROSCI.5465-10.2011) PMID: [21490221](https://pubmed.ncbi.nlm.nih.gov/21490221/).
 21. Etoga JL, Ahmed SK, Patel S, Bridges RJ, Thompson CM. Conformationally-restricted amino acid analogues bearing a distal sulfonic acid show selective inhibition of system $x(c)^-$ over the vesicular glutamate transporter. *Bioorg Med Chem Lett*. 2010; 20(8):2680–3. Epub 2010/03/23. doi: [S0960-894X\(09\)01421-8](https://doi.org/S0960-894X(09)01421-8) [pii] doi: [10.1016/j.bmcl.2009.10.020](https://doi.org/10.1016/j.bmcl.2009.10.020) PMID: [20303751](https://pubmed.ncbi.nlm.nih.gov/20303751/); PubMed Central PMCID: [PMC2860375](https://pubmed.ncbi.nlm.nih.gov/PMC2860375/).
 22. Lo M, Wang YZ, Gout PW. The $x(c)^-$ cystine/glutamate antiporter: a potential target for therapy of cancer and other diseases. *J Cell Physiol*. 2008; 215(3):593–602. Epub 2008/01/09. doi: [10.1002/jcp.21366](https://doi.org/10.1002/jcp.21366) [pii] doi: [10.1002/jcp.21366](https://doi.org/10.1002/jcp.21366) PMID: [18181196](https://pubmed.ncbi.nlm.nih.gov/18181196/).
 23. Patel SA, Rajale T, O'Brien E, Burkhart DJ, Nelson JK, Twamley B, et al. Isoxazole analogues bind the system x_c^- transporter: structure-activity relationship and pharmacophore model. *Bioorg Med Chem*. 2010; 18(1):202–13. Epub 2009/11/26. doi: [S0968-0896\(09\)01009-8](https://doi.org/S0968-0896(09)01009-8) [pii] doi: [10.1016/j.bmc.2009.11.001](https://doi.org/10.1016/j.bmc.2009.11.001) PMID: [19932968](https://pubmed.ncbi.nlm.nih.gov/19932968/); PubMed Central PMCID: [PMC2967674](https://pubmed.ncbi.nlm.nih.gov/PMC2967674/).
 24. Patel SA, Warren BA, Rhoderick JF, Bridges RJ. Differentiation of substrate and non-substrate inhibitors of transport system x_c^- : an obligate exchanger of L-glutamate and L-cystine. *Neuropharmacology*. 2004; 46(2):273–84. Epub 2003/12/19. doi: [S0028390803003460](https://doi.org/S0028390803003460) [pii]. PMID: [14680765](https://pubmed.ncbi.nlm.nih.gov/14680765/).
 25. Shukla K, Thomas AG, Ferraris DV, Hin N, Sattler R, Alt J, et al. Inhibition of x_c^- transporter-mediated cystine uptake by sulfasalazine analogs. *Bioorg Med Chem Lett*. 2011; 21(20):6184–7. Epub 2011/09/06. doi: [S0960-894X\(11\)01027-4](https://doi.org/S0960-894X(11)01027-4) [pii] doi: [10.1016/j.bmcl.2011.07.081](https://doi.org/10.1016/j.bmcl.2011.07.081) PMID: [21889337](https://pubmed.ncbi.nlm.nih.gov/21889337/).
 26. Gout PW, Buckley AR, Simms CR, Bruchofsky N. Sulfasalazine, a potent suppressor of lymphoma growth by inhibition of the $x(c)^-$ cystine transporter: a new action for an old drug. *Leukemia*. 2001; 15(10):1633–40. Epub 2001/10/06. PMID: [11587223](https://pubmed.ncbi.nlm.nih.gov/11587223/).
 27. Wahl C, Liptay S, Adler G, Schmid RM. Sulfasalazine: a potent and specific inhibitor of nuclear factor kappa B. *J Clin Invest*. 1998; 101(5):1163–74. Epub 1998/04/16. doi: [10.1172/JCI992](https://doi.org/10.1172/JCI992) PMID: [9486988](https://pubmed.ncbi.nlm.nih.gov/9486988/); PubMed Central PMCID: [PMC508669](https://pubmed.ncbi.nlm.nih.gov/PMC508669/).
 28. Hosoya K, Tomi M, Ohtsuki S, Takanaga H, Saeki S, Kanai Y, et al. Enhancement of L-cystine transport activity and its relation to xCT gene induction at the blood-brain barrier by diethyl maleate treatment. *J Pharmacol Exp Ther*. 2002; 302(1):225–31. Epub 2002/06/18. PMID: [12065721](https://pubmed.ncbi.nlm.nih.gov/12065721/).
 29. Bannai S. Exchange of cystine and glutamate across plasma membrane of human fibroblasts. *J Biol Chem*. 1986; 261(5):2256–63. Epub 1986/02/15. PMID: [2868011](https://pubmed.ncbi.nlm.nih.gov/2868011/).
 30. Livak KJ, Schmittgen TD. Analysis of relative gene expression data using real-time quantitative PCR and the 2⁻(Delta Delta C(T)) Method. *Methods*. 2001; 25(4):402–8. Epub 2002/02/16. doi: [10.1006/meth.2001.1262](https://doi.org/10.1006/meth.2001.1262) S1046-2023(01)91262-9 [pii]. PMID: [11846609](https://pubmed.ncbi.nlm.nih.gov/11846609/).
 31. Schmittgen TD, Livak KJ. Analyzing real-time PCR data by the comparative C(T) method. *Nat Protoc*. 2008; 3(6):1101–8. Epub 2008/06/13. PMID: [18546601](https://pubmed.ncbi.nlm.nih.gov/18546601/).

32. Nicholls DG, Sihra TS, Sanchez-Prieto J. Calcium-dependent and-independent release of glutamate from synaptosomes monitored by continuous fluorometry. *J Neurochem*. 1987; 49(1):50–7. Epub 1987/07/01. PMID: [2884279](#).
33. McElroy KE, Bouchard PJ, Harpel MR, Horiuchi KY, Rogers KC, Murphy DJ, et al. Implementation of a continuous, enzyme-coupled fluorescence assay for high-throughput analysis of glutamate-producing enzymes. *Anal Biochem*. 2000; 284(2):382–7. Epub 2000/08/31. doi: [10.1006/abio.2000.4740 S0003-2697\(00\)94740-7](#) [pii]. PMID: [10964423](#).
34. Murphy TH, Miyamoto M, Sastre A, Schnaar RL, Coyle JT. Glutamate toxicity in a neuronal cell line involves inhibition of cystine transport leading to oxidative stress. *Neuron*. 1989; 2(6):1547–58. Epub 1989/06/01. doi: [0896-6273\(89\)90043-3](#) [pii]. PMID: [2576375](#).
35. Shih AY, Erb H, Sun X, Toda S, Kalivas PW, Murphy TH. Cystine/glutamate exchange modulates glutathione supply for neuroprotection from oxidative stress and cell proliferation. *J Neurosci*. 2006; 26(41):10514–23. Epub 2006/10/13. doi: [26/41/10514](#) [pii] doi: [10.1523/JNEUROSCI.3178-06.2006](#) PMID: [17035536](#).
36. Chintala S, Li W, Lamoreux ML, Ito S, Wakamatsu K, Sviderskaya EV, et al. Slc7a11 gene controls production of pheomelanin pigment and proliferation of cultured cells. *Proc Natl Acad Sci U S A*. 2005; 102(31):10964–9. Epub 2005/07/23. doi: [0502856102](#) [pii] doi: [10.1073/pnas.0502856102](#) PMID: [16037214](#); PubMed Central PMCID: [PMC1178012](#).
37. Sato H, Shiiya A, Kimata M, Maebara K, Tamba M, Sakakura Y, et al. Redox imbalance in cystine/glutamate transporter-deficient mice. *J Biol Chem*. 2005; 280(45):37423–9. Epub 2005/09/08. doi: [M506439200](#) [pii] doi: [10.1074/jbc.M506439200](#) PMID: [16144837](#).
38. Audi AHW G., Thibault C., Blachot J., Bersillon O. The NUBASE evaluation of nuclear and decay properties. *Nuclear Physics A*. 2003; 729:3–128.
39. Bannai S, Ishii T. Transport of cystine and cysteine and cell growth in cultured human diploid fibroblasts: effect of glutamate and homocysteate. *J Cell Physiol*. 1982; 112(2):265–72. Epub 1982/08/01. doi: [10.1002/jcp.1041120216](#) PMID: [6126484](#).
40. Chung WJ, Sontheimer H. Sulfasalazine inhibits the growth of primary brain tumors independent of nuclear factor-kappaB. *J Neurochem*. 2009; 110(1):182–93. Epub 2009/05/22. doi: [JNC6129](#) [pii] doi: [10.1111/j.1471-4159.2009.06129.x](#) PMID: [19457125](#); PubMed Central PMCID: [PMC3031868](#).
41. Hayes D, Wiessner M, Rauen T, McBean GJ. Transport of L-[14C]cystine and L-[14C]cysteine by subtypes of high affinity glutamate transporters over-expressed in HEK cells. *Neurochemistry international*. 2005; 46(8):585–94. Epub 2005/05/03. doi: [10.1016/j.neuint.2005.03.001](#) PMID: [15863236](#).
42. Dang CV. Glutaminolysis: supplying carbon or nitrogen or both for cancer cells? *Cell Cycle*. 2010; 9(19):3884–6. Epub 2010/10/16. doi: [13302](#) [pii]. PMID: [20948290](#).
43. Le A, Lane AN, Hamaker M, Bose S, Gouw A, Barbi J, et al. Glucose-independent glutamine metabolism via TCA cycling for proliferation and survival in B cells. *Cell Metab*. 2012; 15(1):110–21. Epub 2012/01/10. doi: [S1550-4131\(11\)00468-2](#) [pii] doi: [10.1016/j.cmet.2011.12.009](#) PMID: [22225880](#); PubMed Central PMCID: [PMC3345194](#).
44. Munoz-Pinedo C, El Mjiyad N, Ricci JE. Cancer metabolism: current perspectives and future directions. *Cell Death Dis*. 2012; 3:e248. Epub 2012/01/13. doi: [cddis2011123](#) [pii] doi: [10.1038/cddis.2011.123](#) PMID: [22237205](#); PubMed Central PMCID: [PMC3270265](#).
45. Timmerman LA, Holton T, Yuneva M, Louie RJ, Padro M, Daemen A, et al. Glutamine sensitivity analysis identifies the xCT antiporter as a common triple-negative breast tumor therapeutic target. *Cancer Cell*. 2013; 24(4):450–65. Epub 2013/10/08. doi: [S1535-6108\(13\)00366-8](#) [pii] doi: [10.1016/j.ccr.2013.08.020](#) PMID: [24094812](#); PubMed Central PMCID: [PMC3931310](#).
46. Figuera-Losada M, Rojas C, Slusher BS. Inhibition of microglia activation as a phenotypic assay in early drug discovery. *Journal of biomolecular screening*. 2014; 19(1):17–31. Epub 2013/08/16. doi: [10.1177/1087057113499406](#) PMID: [23945875](#); PubMed Central PMCID: [PMC4111462](#).
47. McMullan SM, Phanavanh B, Li GG, Barger SW. Metabotropic glutamate receptors inhibit microglial glutamate release. *ASN Neuro*. 2012; 4(5). Epub 2012/07/10. doi: [10.1042/AN20120044](#) PMID: [22770428](#); PubMed Central PMCID: [PMC3413012](#).
48. Taylor DL, Diemel LT, Pocock JM. Activation of microglial group III metabotropic glutamate receptors protects neurons against microglial neurotoxicity. *The Journal of neuroscience: the official journal of the Society for Neuroscience*. 2003; 23(6):2150–60. Epub 2003/03/27. PMID: [12657674](#).
49. Barger SW, Goodwin ME, Porter MM, Beggs ML. Glutamate release from activated microglia requires the oxidative burst and lipid peroxidation. *Journal of neurochemistry*. 2007; 101(5):1205–13. Epub 2007/04/04. doi: [10.1111/j.1471-4159.2007.04487.x](#) PMID: [17403030](#); PubMed Central PMCID: [PMC1949347](#).

50. Loane DJ, Stoica BA, Pajoohesh-Ganji A, Byrnes KR, Faden AI. Activation of metabotropic glutamate receptor 5 modulates microglial reactivity and neurotoxicity by inhibiting NADPH oxidase. *The Journal of biological chemistry*. 2009; 284(23):15629–39. Epub 2009/04/15. doi: [10.1074/jbc.M806139200](https://doi.org/10.1074/jbc.M806139200) PMID: [19364772](https://pubmed.ncbi.nlm.nih.gov/19364772/); PubMed Central PMCID: PMC2708859.